Acta Crystallographica Section D
Biological Crystallography
ISSN 0907-4449

Expression, purification, crystallization and preliminary crystallographic analysis of the calponin-homology domain of Rng2

Chern-Hoe Wang,[a]* Martin Walsh,[b] Mohan K. Balasubramanian[c] and Terje Dokland[a]

[a]Institute of Molecular and Cell Biology, 30 Medical Drive, Singapore 117609, Singapore, [b]MRC Grenoble, c/o CRG BM14, ESRF, BP 220, F-38043 Grenoble CEDEX, France, and [c]Temasek Life Sciences Laboratory, 1 Research Link, National University of Singapore, Singapore 117604, Singapore

Correspondence e-mail: chernhoe@imcb.a-star.edu.sg

Received 5 May 2003
Accepted 21 July 2003

Rng2 is a multidomain protein component of the actiomyosin ring and the spindle pole body necessary for cytokinesis in *Schizosaccharomyces pombe*. The calponin-homology domain of Rng2 from *S. pombe* has been overexpressed, purified and crystallized. The crystals belong to space group $P2_1$. Br- and Hg-derivative data sets were measured to 2.21 Å using synchrotron radiation from crystals that were partially fixed with glutaraldehyde. Electron-density maps have been obtained from two-wavelength MAD on the Br derivative and SAD on the Hg derivative.

1. Introduction

Cytokinesis is an essential process in which a cell with newly divided nuclei cleaves to form two daughter cells. Underlying this process is a contraction of the cytokinetic actomyosin ring powered by the motor activity of a type II myosin (Schroeder, 1973). The fission yeast *Schizosaccharomyces pombe* is an excellent model organism to study cytokinesis since it achieves cell division using a medially placed actomyosin ring, which is functionally similar to the mammalian cleavage furrow. Besides, its genome is fully sequenced and this facilitates gene identification and genetic manipulation. The fission yeast actomyosin ring assembles at the medial cortex during metaphase, constricts after anaphase B to guide the centripetal deposition of the septum and is disassembled at the end of cytokinesis. At least 20 mutants have been implicated in cytokinesis. They can be classified into three major classes: those affecting cleavage-plane specification [*pom1* (Bahler & Pringle, 1998), *mid1* (Chang *et al.*, 1996; Sohrmann *et al.*, 1996) and *plo1* (Bahler *et al.*, 1998)], those controlling actin-ring assembly [*cdc3*, *cdc4*, *cdc8*, *cdc12* (Nurse *et al.*, 1976; Chang *et al.*, 1996), *myo2* (Kitayama *et al.*, 1997; May *et al.*, 1997), *rng2* (Eng *et al.*, 1998) and *rng3* (Wong *et al.*, 2000)] and those regulating actin-ring contraction and/or septum deposition at the end of mitosis [*cdc7* (Fankhauser *et al.*, 1994), *cdc11*, *cdc14* (Fankhauser *et al.*, 1993), *spg1* (Schmidt *et al.*, 1997), *sid1*, *sid2*, *sid4* (Balasubramanian *et al.*, 1998) and *mob1* (Hou *et al.*, 2000)].

The *S. pombe rng2*$^+$ gene encodes a 172 kDa protein with 1489 amino-acid residues. BLAST analysis (Altschul *et al.*, 1990) shows a top match to mouse Iqgap1, with a sequence identity of 30% and a sequence similarity of 51%. RPS-BLAST analysis (Altschul *et al.*, 1997) reveals matches to a calponin-homology (CH) domain in the N-terminus, a rasGAP domain and a rasGAP C-terminal domain. Coiled-coil prediction (Lupas *et al.*, 1991) suggests the presence of two coiled-coil domains at residues 734–767 and at residues 1334–1362. Hidden Markov model (HMM) analysis (Eddy, 1998) using a calibrated profile HMM constructed from aligned IQ motifs reveals the presence of 11 such IQ repeats within Rng2.

The function of the Rng2 CH domain in fission yeast is unclear. However, it is known that Rng2 requires F-actin for its localization to the actomyosin ring (Eng *et al.*, 1998). To clarify the nature of the CH domain, we have initiated X-ray crystallographic studies and here we report the crystallization and preliminary crystallographic data analysis of Rng2-CH.

2. Methods and results

2.1. Expression

The DNA segment coding for protein residues 1–190 of *rng2* (gene *SPAC4F8.13c*, GenBank accession No. NP_593860.1) was amplified from the pREP4X-GST-*rng2* (pCDL 222.1) construct containing the full-length *rng2* sequence using the 5′ primer GAC GAC GAA TTC ATG GAC GTA AAT GTG GGA and the 3′ primer GCG CCG GAG CTC TCA TAA AGC TTT GAA GTT AGG. Residues 1–190 of Rng2 contain the calponin-homology domain (Rng2-CH). The PCR product was cloned into the *Eco*RI and *Sca*I sites of the pGEX-KG expression vector (Guan & Dixon, 1991). The pGEX-KG vector was developed for the expression of proteins with an N-terminal fusion to a glutathione *S*-transferase (GST) tag. There is a 19-amino-acid residue linker (SDLVPR^GSPGISGGGGGIL) separating the GST domain from the Rng2-CH domain. It has a glycine-rich sequence PGISGGGGG immediately after the thrombin-cleavage site

that increases the thrombin-cleavage efficiency (Guan & Dixon, 1991). The linker is cleaved by thrombin at the indicated site between arginine and glycine.

Plasmids were transformed into *Escherichia coli* BL21-CodonPlus-RIL {F$^-$ *ompT hsdS*(r_B^- m_B^-) *dcm*$^+$ *Tet*^{r} *gal endA Hte* [*argU ileY leuW Cam*^{r}]}from Stratagene and sequenced. A 0.5 ml aliquot of freshly saturated cells was mixed with an equal portion of a cryoprotectant consisting of 65% glycerol, 0.1 *M* $MgSO_4$, 25 m*M* Tris pH 8 and frozen at 193 K. For the purpose of protein production, freshly thawed cells were inoculated into 50 ml of Luria–Bertani (LB) media supplemented with 100 µg ml^{-1} ampicillin and grown in a shaker for 7 h at 310 K. A 10 ml aliquot was then used to inoculate 1 l of 2×YT media in a 5 l Erlenmeyer flask and induced with 0.5 m*M* IPTG at A_{600} = 0.6. The cells were harvested 3 h later by centrifugation (4500*g* for 10 min), resuspended in 5 ml of cold PBS pH 7.4, 2 m*M* DTT and homogenized in a cold pressure cell with a French press (Thermo Spectronic) operated at a gauge pressure of 10.3 MPa. 10 µg ml^{-1} DNase and RNase was added to the lysate and incubated for 30 min at 277 K on a rocking platform. Centrifugation at 10 000*g* for 20 min was used to separate the supernatant from the pellet, which was discarded. The supernatant was clarified using a 0.45 µm filter.

2.2. Purification

The GST-Rng2-CH fusion protein was bound to a 5 ml GSTrap FF column (Pharmacia), washed with 20 m*M* Tris pH 8, 0.5 *M* NaCl and eluted with 50 m*M* Tris, 10 m*M* reduced glutathione pH 8. 50 units of thrombin were added to the eluate and incubated overnight at 277 K. The fusion protein was cleaved efficiently (Fig. 1). The eluate was dialyzed into 20 m*M* Tris, 0.5 *M* NaCl using a 3500 Da molecular-weight cutoff dialysis tubing (Pierce). Thrombin and the cleaved GST were removed by passing through a 5 ml HiTrap benzamidine FF (Pharmacia) column and a 5 ml GSTrap FF column that was connected in series. Rng2-CH was concentrated to 15 mg ml^{-1} in 50 m*M* Tris pH 8, 0.15 *M* NaCl, 2.5 m*M* $CaCl_2$ with centrifugal filter devices from Amicon.

2.3. Crystallization

Crystallization screens of Rng2-CH were initially performed with commercially available solutions (Wizard I and II; deCODE Genetics) using the sitting-drop vapour-diffusion method. Crystallization setups contained 2 µl of Rng2-CH protein solution (15 mg ml^{-1} in 50 m*M* Tris pH 8, 0.15 *M* NaCl, 2.5 m*M* $CaCl_2$) and 2 µl of Wizard I/II solution. The wells were sealed with clear sealing tape (Hampton Research). A rod-shaped crystal was observed in one well from the Wizard II screen. This condition was optimized slightly by exploring different precipitant concentrations (18–21% PEG), precipitants (PEG 3000 and 4000), salt concentrations (0.2–0.3 *M* calcium acetate) and buffer pHs (pH 7–7.5). Up to five monoclinic crystals of Rng2-CH appeared in each sitting-drop well with 21% PEG 3000, 0.3 *M* calcium acetate and 0.1 *M* Tris pH 7 after incubation at room temperature (295 K) for 8 d. They grew to maximal dimensions (0.3 × 0.2 × 0.05 mm) within two weeks (Fig. 2).

2.4. Collection and processing of X-ray diffraction data

The crystals were first transferred into the reservoir buffer solution in order to remove the precipitate. This was followed by 15 min fixation in 21% PEG 3000, 3% glutaraldehyde at 288 K in a sitting-drop tray. This brief fixation prevents crystals with dimensions greater than 0.2 mm from cracking across the unique axis while soaking in cryobuffer or in derivatization solutions (Fitzpatrick *et al.*, 1994). Our fixation protocol was modified by doubling the glutaraldehyde concentration and shortening the fixation times since our crystals did not diffract after overnight fixation (unpublished observations). In contrast, extended cross-linking times of a day or more with lysozyme crystals did not make the crystals disordered (Wang *et al.*, 1998).

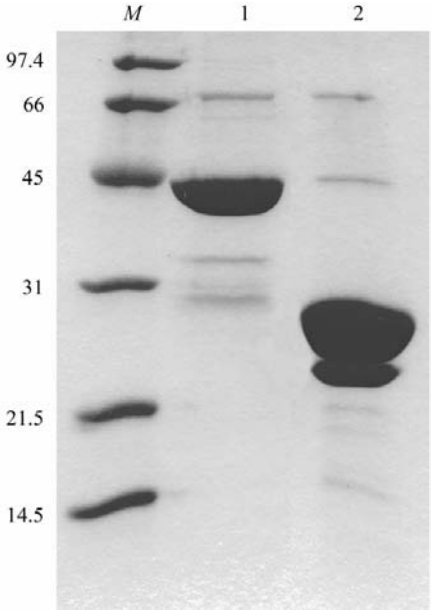

Figure 1
Thrombin cleavage of GST-Rng2-CH. Lane *M*, molecular-weight standards; lane 1, before cleavage; lane 2, after overnight cleavage with thrombin.

The native crystals were soaked in a cryobuffer containing 21% PEG 3000, 40% glycerol. Bromide derivatives were soaked for 30 min in 21% PEG 3000, 25% glycerol, 1 *M* NaBr. Mercury derivatives were soaked for 2 h in saturated $HgCl_2$, 40% glycerol. The crystals were mounted on nylon loops, frozen in liquid nitrogen and transported to the synchrotron in a dry shipping dewar (Taylor-Wharton CP-100) for data collection at the European Synchrotron Radiation Facility (ESRF).

X-ray diffraction data from Rng2-CH were measured under cryogenic conditions at the UK/EMBL MAD beamline BM14 at the ESRF using a MAR CCD 165 mm detector (MAR USA). The data set (Table 1) was collected as a continuous series of 2° oscillation images covering a rotation range of 200°. Indexing and integration of the images was performed using *DENZO* and scaling of the intensity data was performed using *SCALEPACK* from the *HKL* package (Otwinowski & Minor, 1997).

2.5. Structure determination

A three-wavelength MAD data set for the Br derivative was collected. We found that the inflection and remote wavelengths had sufficient anomalous signal to perform two-wavelength MAD (González, 2003). This served as input data to *SHELXD* (Sheldrick, 1998) after extracting Bijvoet differences using *XPREP* (Bruker). *SHELXD* was run with 388 *E* values greater than 1.5, looking for four anomalous sites. The ten highest peaks with a correlation coefficient (CC) of 38.41 and a figure-of-merit (PATFOM) of 46.95 were accepted for further refinement and phasing by *SHARP* (de La Fortelle & Bricogne, 1997). The map obtained after

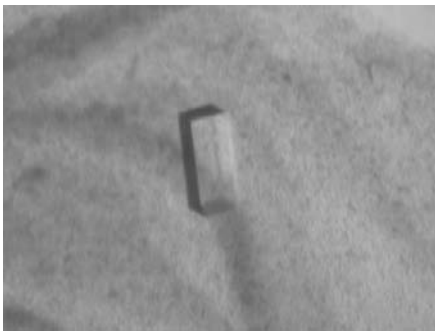

Figure 2
Crystals of Rng2-CH. They typically measure 200 µm in the longest dimension.

Table 1
Data-collection and processing statistics of monoclinic crystals of Rng2-CH.

Values in parentheses are for the highest resolution shell.

	Rng2-CH + 1 *M* NaBr	Rng2-CH + saturated $HgCl_2$
Space group	$P2_1$	$P2_1$
Crystal dimensions (mm)	0.3 × 0.2 × 0.05	0.3 × 0.2 × 0.05
Unit-cell parameters		
a (Å)	31.266	30.884
b (Å)	68.836	68.666
c (Å)	39.811	35.309
$\alpha = \gamma$ (°)	90	90
β (°)	105.544	102.514
V_M (Å^3 Da^{-1})	2.3	2.0
Solvent content (%)	46.3	39.3
Molecules per AU	1	1
Diffraction source	ESRF BM14	ESRF BM14
Wavelength (Å)	Peak, 0.919087; inflection, 0.919338; remote, 0.855057	1.653
Resolution (Å)	2.21 (2.29–2.21)	2.21 (2.29–2.21)
No. of observations	25342	130550
No. of independent reflections	7347 (202)	7034 (570)
R_{merge} (%)	5.3 (7.7)	8.4 (14.5)
Completeness (%)	89.6 (24.8)	97.4 (81.5)
$I/\sigma(I)$	20.43 (9.39)	32.70 (9.93)

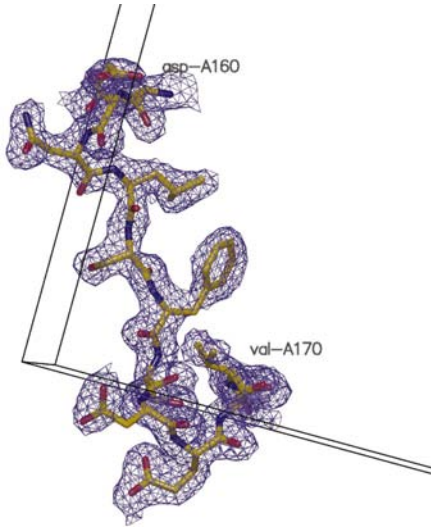

Figure 3
A representative section of the two-wavelength Br MAD σ_A map of Rng2-CH calculated at 2.21 Å resolution and displayed at a cutoff of 1σ. The map is superimposed on an atomic model of the structure together with the unit cell.

density modification was readily interpretable: 147 of 159 residues could be built automatically using *wARP* (Perrakis *et al.*, 1999). A SAD data set was also collected for the Hg derivative at a wavelength of 1.653 Å. We found a strong anomalous signal even though the L_{III} wavelength is around 1 Å. *SHELXD* was run with 391 *E* values greater than 1.5, looking for three anomalous sites. The five highest peaks with a CC of 46.67 and a PATFOM of 100.97 were further refined and phased as above. 148 of 159 residues could be built with *wARP*. Both structures are currently being refined (Fig. 3). The glycine-rich linker and residues 1–31 of Rng2 were disordered and were not visible in both maps.

2.6. Discussion

CH domains may exist either in pairs as an actin-binding domain (ABD) or alone in actin-binding proteins. Experimental evidence for actinin (Kuhlman *et al.*, 1992), dystrophin (Way *et al.*, 1992), filamin (Lebart *et al.*, 1994), fimbrin/plastin (Hanein *et al.*, 1997,1998), MACF (Leung *et al.*, 1999), plectin (García-Alvarez *et al.*, 2003), spectrin (Karinch *et al.*, 1990) and utrophin (Winder *et al.*, 1995) shows that the ABD can bind F-actin in isolation.

The CH domain exists singly in several proteins that have F-actin-binding activity such as calponin (Gimona & Mital, 1998), IQGAP1 (Bashour *et al.*, 1997; Fukata *et al.*, 1997; Ho *et al.*, 1999) and SM22 (Fu *et al.*, 2000). However, the evidence suggests that the CH domain of calponin and SM22 is unable to bind F-actin in isolation. Calponin and SM22 both bind F-actin through their C-terminal repeats and not *via* the N-terminal CH domain (Gimona & Mital, 1998; Fu *et al.*, 2000). On the other hand, IQGAP proteins such as Rng2 do not have any recognizable C-terminal repeats equivalent to those found in calponin and SM22. Either the CH domain or some unknown C-terminal sequences could be responsible for the F-actin-binding activity of Rng2. Single CH domains are quite dissimilar in terms of their amino-acid sequence and this probably allows functional diversity (Stradal *et al.*, 1998). Thus, some CH domains may have secondarily lost their ability to bind F-actin, such as in the case of calponin and SM22.

We have obtained crystals of an N-terminal fragment of Rng2 where residues 32–190 are visible in the electron-density map. The CH domain lies between residues 40 and 150, but our structure extends from residues 32 to 190. We hope that by combining these data with functional information inferred from *S. pombe* genetics, we will be able to further clarify its actin-binding properties and its biological context.

We would like to thank the EMBL Grenoble Outstation for providing support for measurements at the ESRF under the European Union 'Improving Human Potential Programme'.

References

Altschul, S. F., Gish, W., Miller, W., Myers, E. W. & Lipman, D. J. (1990). *J. Mol. Biol.* **215**, 403–410.
Altschul, S. F., Madden, T. L., Schaffer, A. A., Zhang, J., Zhang, Z., Miller, W. & Lipman, D. J. (1997). *Nucleic Acids Res.* **25**, 3389–3402.
Bahler, J. & Pringle, J. R. (1998). *Genes Dev.* **12**, 1356–1370.
Bahler, J., Steever, A. B., Wheatley, S., Wang, Y., Pringle, J. R., Gould, K. L. & McCollum, D. (1998). *J. Cell Biol.* **143**, 1603–1616.
Balasubramanian, M. K., McCollum, D., Chang, L., Wong, K. C., Naqvi, N. I., He, X., Sazer, S. & Gould, K. L. (1998). *Genetics*, **149**, 1265–1275.
Bashour, A. M., Fullerton, A. T., Hart, M. J. & Bloom, G. S. (1997). *J. Cell Biol.* **137**, 1555–1566.
Chang, F., Wollard, A. & Nurse, P. (1996). *J. Cell Sci.* **109**, 131–142.
Eddy, S. R. (1998). *Bioinformatics*, **14**, 755–763.
Eng, K., Naqvi, N. I., Wong, K. C. Y. & Balasubramanian, M. K. (1998). *Curr. Biol.* **8**, 611–621.
Fankhauser, C. & Simanis, V. (1993). *Mol. Biol. Cell*, **4**, 531–539.
Fankhauser, C. & Simanis, V. (1994). *EMBO J.* **13**, 3011-3019.
Fitzpatrick, P. A., Ringe, D. & Klibanov, A. M. (1994). *Biochem. Biophys. Res. Commun.* **198**, 675–681.
Fu, Y., Liu, H. W., Forsythe, S. M., Kogut, P., McConville, J. F., Halayko, A. J., Camoretti-Mercado, B. & Solway, J. (2000). *J. Appl. Physiol.* **89**, 1985–1990.
Fukata, M., Kuroda, S., Fujii, K., Nakamura, T., Shoji, I., Matsuura, Y., Okawa, K., Iwamatsu, A., Kikuchi, A. & Kaibuchi, K. (1997). *J. Biol. Chem.* **272**, 29579–29583.
García-Alvarez, B., Bobkov, A., Sonnenberg, A. & de Pereda, J. M. (2003). *Structure*, **11**, 615–625.
Gimona, M. & Mital, R. (1998). *J. Cell Sci.* **111**, 1813–1821.
González, A. (2003). *Acta Cryst.* D**59**, 315–322.
Guan, K. L. & Dixon, J. E. (1991). *Anal. Biochem.* **192**, 262–267.
Hanein, D., Matsudaira, P. & DeRosier, D. J. (1997). *J. Cell Biol.* **139**, 387–396.
Hanein, D., Volkmann, N., Goldsmith, S., Michon, A. M., Lehman, W., Craig, R., DeRosier, D., Almo, S. & Matsudaira, P. (1998). *Nature Struct. Biol.* **5**, 787–792.
Ho, Y. D., Joyal, J. L., Li, Z. & Sacks, D. B. (1999). *J. Biol. Chem.* **274**, 464–470.
Hou, M. C., Salek, J. & McCollum, D. (2000). *Curr. Biol.* **10**, 619–622.
Karinch, A. M., Zimmer, W. E. & Goodman, S. R. (1990). *J. Biol. Chem.* **265**, 11833–11840.
Kitayama, C., Sugimoto, A. & Yamamoto, M. (1997). *J. Cell Biol.* **137**, 1309–1319.
Kuhlman, P. A., Hemmings, L. & Critchley, D. R. (1992). *FEBS Lett.* **304**, 201–206.
La Fortelle, E. de & Bricogne, G. (1997). *Methods Enzymol.* **276**, 472–494.
Lebart, M. C., Mejean, C., Casanova, D., Audemard, E., Derancourt, J., Roustan, C. & Benyamin, Y. (1994). *J. Biol. Chem.* **269**, 4279–4284.
Leung, C. L., Sun, D., Zheng, M., Knowles, D. R. & Liem, R. K. (1999). *J. Cell Biol.* **147**, 1275–1286.
Lupas, A., Van Dyke, M. & Stock, J. (1991). *Science*, **252**, 1162–1164.

May, K. M., Watts, F. Z., Jones, F. Z. & Hyams, J. S. (1997). *Cytoskeleton*, **38**, 1–12.
Nurse, P., Thuriaux, P. & Nasmyth, K. (1976). *Mol. Gen. Genet.* **146**, 167–178.
Otwinowski, Z. & Minor, W. (1997). *Methods Enzymol.* **276**, 307–327.
Perrakis, A., Morris, R. & Lamzin, V. S. (1999). *Nature Struct. Biol.* **6**, 458–463.
Schmidt, S., Sohrmann, M., Hofmann, K., Wollard, A. & Simanis, V. (1997). *Genes Dev.* **11**, 1519–1534.
Schroeder, T. E. (1973). *Proc. Natl Acad. Sci. USA*, **70**, 1688–1692.
Sheldrick, G. M. (1998). *Direct Methods for Solving Macromolecular Structures*, edited by S. Fortier, pp. 401–411. Dordrecht: Kluwer Academic Publishers.
Sohrmann, M., Fankhauser, C., Brodbeck, C. & Simanis, V. (1996). *Genes Dev.* **10**, 2707–2719.
Stradal, T., Kranewitter, W., Winder, S. J. & Gimona, M. (1998). *FEBS Lett.* **431**, 134–137.
Wang, Z., Zhu, G., Huang, Q., Qian, M., Shao, M., Jia, Y. & Tang, Y. (1998). *Biochim. Biophys. Acta*, **1384**, 335–344.
Way, M., Pope, B., Cross, R. A., Kendrick-Jones, J. & Weeds, A. G. (1992). *FEBS Lett.* **301**, 243–245.
Winder, S. J., Hemmings, L., Maciver, S. K., Bolton, S. J., Tinsley, J. M., Davies, K. E., Critchley, D. R. & Kendrick-Jones, J. (1995). *J. Cell Sci.* **108**, 63–71.
Wong, K. C. Y., Naqvi, N. I., Lino, Y., Yamamoto, M. & Balasubramanian, M. K. (2000). *J. Cell Sci.* **113**, 2421–2432.